Spin-transfer-torque-induced rf oscillations in CoFeB/MgO/CoFeB magnetic tunnel junctions under a perpendicular magnetic field

T. Wada,[1] T. Yamane,[1] T. Seki,[1,*] T. Nozaki,[1] Y. Suzuki,[1,2] H. Kubota,[2] A. Fukushima,[2] S. Yuasa,[2] H. Maehara,[3] Y. Nagamine,[3] K. Tsunekawa,[3] D. D. Djayaprawira,[3] and N. Watanabe[3]

[1]*Graduate School of Engineering Science, Osaka University, 1-3 Machikaneyama-cho, Toyonaka, Osaka 560-8531, Japan*

[2]*Nanoelectronics Research Institute (NeRI), National Institute of Advanced Industrial Science and Technology (AIST), 1-1-1, Umezono, Tsukuba 305-8568, Japan*

[3]*Electron Device Division, Canon ANELVA Corporation, 5-1-2 Kurigi, Asao, Kawasaki-shi, Kanagawa 215-8550, Japan*

(Received 17 October 2009; revised manuscript received 11 January 2010; published 15 March 2010)

We investigated spin-transfer-torque (STT)-induced rf oscillation with a magnetic field applied perpendicular to the plane of CoFeB/MgO/CoFeB magnetic tunnel junctions (MTJs). For the rf measurement with the magnetic field normal to the MTJ plane, the magnetic field dependence of the peak frequency (f_0), the linewidth (Δf), and the power spectral density (PSD) were well interpreted as behavior in a linear regime, which showed the minima of f_0 and Δf and the maximum of PSD at the demagnetizing field of the free layer. However, no clear onset of STT-induced rf oscillation was observed even with a large bias current applied. Under the magnetic field slightly tilted from the normal direction, on the other hand, the spectral shape strongly depended on the bias current. With the current in the direction to stimulate STT-induced rf oscillation, a rapid blueshift of f_0 and an abrupt increase in PSD were observed together with a remarkable broadening of Δf, indicating that STT-induced rf oscillation was achieved. The critical current for STT-induced rf oscillation estimated from the variation in Δf was also in good agreement with the bias current at which the peak of the second harmonics of f_0 appeared in the rf spectrum.

DOI: 10.1103/PhysRevB.81.104410 PACS number(s): 85.75.−d, 72.25.−b

I. INTRODUCTION

Spin-polarized current passing through a device comprising a magnetic free layer and a spin-polarizing layer separated by a nonmagnetic metal or thin insulating layer gives rise to a torque on the local magnetization vectors. This torque is called the "spin-transfer-torque (STT)," originating from the spin angular momentum transfer from the conduction electron spin to the local spin,[1,2] and this enables us to manipulate the local magnetization direction without an external magnetic field. STT acts to enhance or suppress the intrinsic magnetization damping torque depending on the direction of the current flow and the magnetization directions of the free and spin-polarizing layers. In certain conditions in which STT overcomes the intrinsic damping torque, magnetization reversal of the free layer occurs. When STT and the intrinsic damping torque are balanced, the magnetization shows a steady precession, which is called the STT-induced rf oscillation. This rf oscillation of magnetization was first observed in all-metallic multilayers,[3–5] and many investigations have been done to clarify the magnetic dynamics and to realize potential applications such as a microwave oscillator.[6–9]

A magnetic tunnel junction (MTJ) with a MgO barrier showing a large tunnel magnetoresistance (TMR) effect[10–12] is a key for such applications since the large MR ratio leads to large rf output power. Recently, several studies on STT-induced rf oscillation have been reported using MgO-based MTJs.[13–18] Compared with all-metallic multilayer systems, however, there are several difficulties in observing STT-induced rf oscillation for MTJs. One of the serious problems is deterioration or dielectric breakdown of the thin tunnel barrier during the measurement because a large bias voltage is applied to inject current of the order of 10^6 A/cm^2, which sometimes leads to low reproducibility in the experimental results. Although it has been reported that low-resistance MTJs with a relatively low TMR ratio easily exhibit STT-induced rf oscillation compared with high-resistance MTJs, the reason for this and the detail mechanism are still not clear.[15–17] The shape of the rf spectrum, which includes multiple peaks,[13] is also a problem, implying the existence of several precessional modes and is an obstacle to a precise analysis. In addition, the large thermal noise enhanced by STT makes it difficult to clearly determine the onset of STT-induced rf oscillation. Thus, it is first necessary to suppress the additional precessional modes and to make the shape of the rf spectrum a single peak structure for high-quality MgO-based MTJs with a high TMR ratio. Then, it is important to determine the critical current for the onset of STT-induced rf oscillation.

Here, we present STT-induced rf oscillation with a magnetic field applied perpendicular to the plane of MgO-based MTJs. This perpendicular magnetic field is expected to suppress the additional precessional modes since it leads to a uniform demagnetization field in the nanosized pillar of the MTJ in comparison with the in-plane magnetic field. The magnetic field and the bias current dependences of the peak frequency (f_0), the linewidth (Δf), and the power spectral density (PSD) of the rf spectrum are investigated. In this paper, the device structure and the measurement setup are described in Sec. II. Section III is devoted to the results when a magnetic field is applied normal to the MTJ plane. Section IV shows STT-induced rf oscillation with the magnetic field slightly tilted from the normal to the MTJ plane. The experimental results are also discussed based on a theory for nonlinear auto-oscillators.

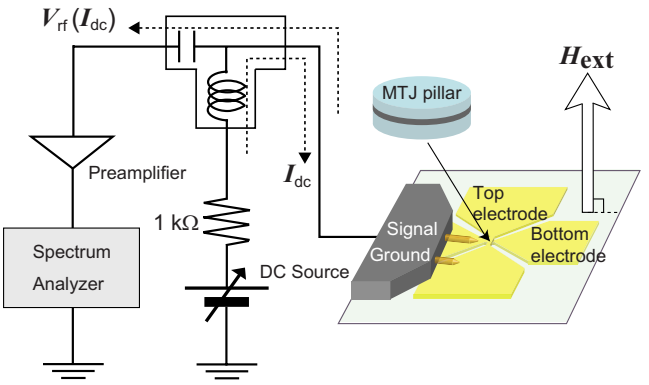

FIG. 1. (Color online) Schematic illustration of the device and the measurement setup for the rf spectrum. The external magnetic field (H_{ext}) was applied in the perpendicular direction to the plane of the MTJ.

II. EXPERIMENTAL PROCEDURES

A MTJ film with the following stacked structure was prepared by sputter deposition: thermally oxidized Si wafer/buffer layers/PtMn (15 nm)/CoFe (2.5 nm)/Ru (0.85 nm)/CoFeB (3 nm)/Mg (0.6 nm)/MgO (0.6 nm)/CoFeB (2 nm)/capping layers. The buffer layers consist of CuN and Ta layers. The 2-nm-thick CoFeB layer is a free layer. The composition of the CoFeB layers is Co:Fe:B=60:20:20. A Mg layer with the thickness of 0.6 nm was inserted between the 3-nm-thick CoFeB pinned layer and the 0.6-nm-thick MgO tunnel barrier to obtain a high MR ratio and a low resistance-area (RA) product.[19] The MTJ film was patterned into a pillar-shaped structure with an elliptical cross section of 70 $\times$160 nm^2 by a combination of electron beam lithography, ion milling, and lift-off techniques.

Figure 1 schematically illustrates the device and the measurement setup. The MTJ pillar is placed at the intersection of the top and bottom electrodes. The MR measurement was performed at room temperature using a conventional two-terminal technique with a bias voltage of 10 mV applied. The frequency-domain measurement was carried out using a spectrum analyzer. The MTJ device was connected to the circuit with a two-terminal rf probe and a dc bias current (I_{dc}) was applied from a dc power source through a bias-Tee. The STT-induced rf oscillation generates a high-frequency voltage output signal [$V_{rf}(I_{dc})$] due to the time variation in resistance originating from the TMR effect. Output signals amplified by a preamplifier were fed to a spectrum analyzer. All the rf measurements were performed at room temperature. The positive I_{dc} is defined as the direction of the electron flow from the free layer to the pinned one. The background signal at I_{dc}=0 mA was subtracted from the measured rf spectra. PSD for the present measurement is expressed as

$$\mathrm{PSD} = \left(\frac{1}{G_{\mathrm{preamp}}}\right)^2 \frac{V_{\mathrm{rf}}(I_{\mathrm{dc}})^2}{Z_0 \Delta f_{\mathrm{RB}}} \ [\mathrm{W/Hz}], \qquad (1)$$

where G_{preamp}, Z_0, and Δf_{RB} denote the frequency-dependent gain of the preamplifier, the characteristic impedance (50 Ω), and the resolution bandwidth of the spectrum analyzer (3 MHz), respectively.

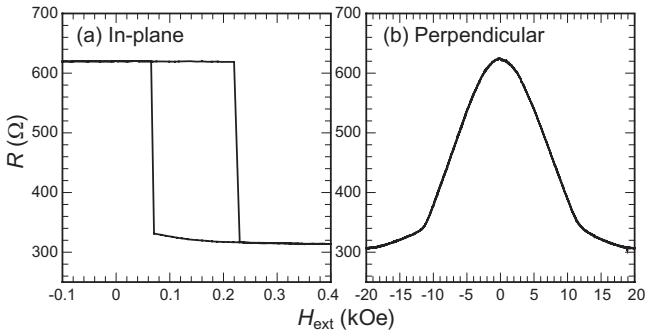

FIG. 2. MR curves measured with (a) the in-plane easy-axis magnetic field and (b) the perpendicular magnetic field. The direction of the perpendicular magnetic field is strictly along the normal to the MTJ plane. A bias voltage of 10 mV was applied.

III. rf SPECTRA UNDER A PERPENDICULAR MAGNETIC FIELD

Figure 2(a) shows a MR curve with an external magnetic field (H_{ext}) applied along the in-plane easy-axis direction of the MTJ. The MR ratio which is defined as $(R_{AP}-R_P)/R_P$ (where R_{AP} and R_P are the resistance values of the antiparallel and parallel alignments of the magnetizations) is ~100% and the RA value in the parallel state is ~2.3 Ω μm^2 for the present device. Figure 2(b) shows a MR curve with H_{ext} applied normal to the plane of the MTJ. At H_{ext}=0 Oe, the antiparallel alignment is stable due to the dipole interaction between the free and pinned layers. The resistance of the MTJ gradually decreases as H_{ext} increases, which means the continuous change in the magnetic configuration from the antiparallel to the parallel alignment. An important point is that the measured MR curve is completely symmetric with respect to the zero magnetic field, indicating that H_{ext} is applied strictly normal to the MTJ plane.

rf spectra at various H_{ext} normal to the MTJ plane are shown in Fig. 3. Although I_{dc}=0.1 mA is small enough to neglect the effect of STT, a clear single peak structure was observed in a wide range of H_{ext}. Such an explicit peak structure enables us to precisely analyze the magnetic field and the bias current dependences of f_0, Δf, and PSD. Figures 4(a)–4(c) show f_0, Δf, and PSD as a function of H_{ext}, respectively. I_{dc} was fixed at 0.1 mA. As H_{ext} increases, f_0 gradually decreases and reaches a minimum at H_{ext}=11 kOe, and then increases linearly for H_{ext}>11 kOe. Δf also shows a minimum value around H_{ext}=11 kOe, whereas PSD shows a maximum. The peaks observed in the rf spectra originate from the thermally excited ferromagnetic resonance (FMR) mode of the free layer. The decrease in f_0 is due to the continuous change from the in-plane precession to the out-of-plane precession and the magnetization direction is aligned to the normal axis of the MTJ plane in the magnetic field region where f_0 increases linearly. These magnetic field dependences of f_0 and Δf are interpreted as behavior in the linear regime. Using Kittel's FMR formula,[20] f_0 under a perpendicular magnetic field is expressed as[21]

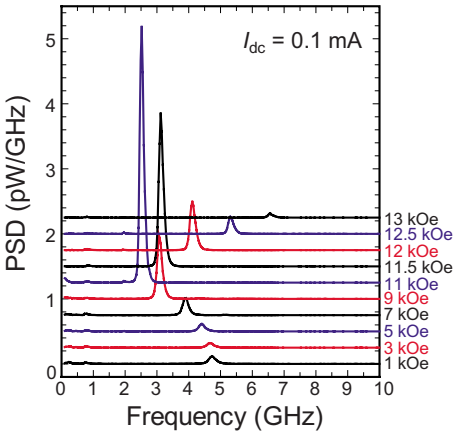

FIG. 3. (Color online) rf spectra at various external magnetic fields (H_{ext}). The external magnetic field was applied along the normal to the MTJ plane. The bias current (I_{dc}) was fixed at 0.1 mA. For clarity, the spectra have been shifted vertically.

$$f_0 = \begin{cases} \dfrac{\gamma}{2\pi}\sqrt{H_c H_d\left(1-\dfrac{H_{ext}^2}{H_d^2}\right)} & H_{ext} < H_d \\ \dfrac{\gamma}{2\pi}\sqrt{(H_{ext}-H_d)(H_{ext}-H_d+H_c)} & H_d < H_{ext}, \end{cases} \tag{2}$$

where H_c and H_d denote the coercivity and the demagnetizing field, respectively. γ is the gyromagnetic ratio. It is found that the experimental data are well fitted by Eq. (2). From the result of the fitting [the dashed line in Fig. 4(a)], $H_c \sim 240$ Oe and $H_d \sim 11.08$ kOe are obtained. Using the value of H_d, saturation magnetization (M_s) for the CoFeB free layer is calculated to be ~ 880 emu/cm^3, which is lower than 1100 emu/cm^3.[22] This discrepancy suggests that perpendicular magnetic anisotropy exists in the CoFeB free layer as a previous paper reported.[21] Δf at $H_{ext}=0$ Oe is given by $\Delta f = \alpha(\gamma/2\pi)[H_c+H_d]$, where α is the damping parameter. In this study, α is calculated to be 0.009 using $\Delta f \sim 300$ MHz, $H_c \sim 240$ Oe, and $H_d \sim 11.08$ kOe. This value of α is almost equal to the value used in the STT-induced switching measurement.[22] Since PSD shows a maximum around $H_{ext}=11$ kOe, the precessional angle of magnetization becomes large when H_{ext} is comparable to H_d.

Figures 5(a) and 5(b) show f_0 and Δf as a function of I_{dc}, respectively. H_{ext} was fixed at 10 kOe. The relative angle between the free and the fixed layers was $\sim 60°$. The positive I_{dc} is the current direction stimulating the rf oscillation (which is labeled the "antidamping side"), and the negative one is that constricting the magnetization precession (which is labeled the "forced side"). In the high bias current region, f_0 shifts due to the effect of STT [Fig. 5(a)]. f_0 shows a blueshift on the forced side whereas it shows a redshift on the antidamping side. The blueshift (redshift) indicates that the precessional angle becomes smaller (larger) due to STT. According to a theory proposed by Kim *et al.*,[23] Δf decreases linearly with increasing I_{dc} in the linear regime. The linear decrease in Δf means that the effective damping is reduced by STT. The I_{dc} dependence of Δf in the linear regime is simply expressed as

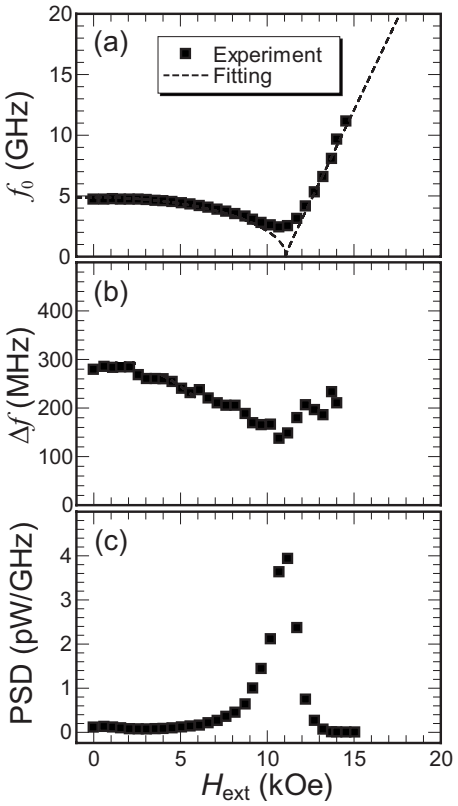

FIG. 4. External magnetic field (H_{ext}) dependence of (a) peak frequency (f_0), (b) linewidth (Δf), and (c) the PSD. The bias current (I_{dc}) was fixed at 0.1 mA. The external magnetic field was applied along the normal to the MTJ plane. The dashed line in (a) is the result of fitting using Eq. (2).

$$\Delta f = \frac{\sigma}{2\pi}(I_{c0} - I_{dc}), \tag{3}$$

where σ is the spin-polarization efficiency defined by Eq. (5) in Ref. 24 and I_{c0} is the critical current for the onset of STT-induced rf oscillation. The value of I_{c0} is estimated by linearly extrapolating Δf to zero. This linear dependence has been observed in other reports at low bias currents.[15,16,25,26] In this measurement, the linear relationship is observed in the negative I_{dc} region, indicating that the STT supports the magnetization damping in the negative I_{dc}. On the other hand, Δf at the positive I_{dc} shows the deviation from the linear relationship. Although it is not clear why the variation in Δf deviates from the linear relationship even at the low I_{dc}, the transition from a linear to a nonlinear regime might occur due the STT. I_{c0} is estimated to be 3.6 mA for this measurement condition from the linear extrapolation [the dashed line in Fig. 5(b)]. This value of I_{c0} is much higher than the maximum I_{dc} applied in the experiment. Figure 5(c) shows I_{dc} versus PSD. At the low I_{dc} region from -1.7 to 1.7 mA, PSD shows a quadratic increase. This is because the values of PSD are not normalized by I_{dc}.[2] The output power due to the thermally excited ferromagnetic resonance mode shows the quadratic increase with I_{dc}. However, PSD for the forced side decreases at $I_{dc} < -1.7$ mA, implying that STT reduces the precessional angle. In contrast, the quadratic in-

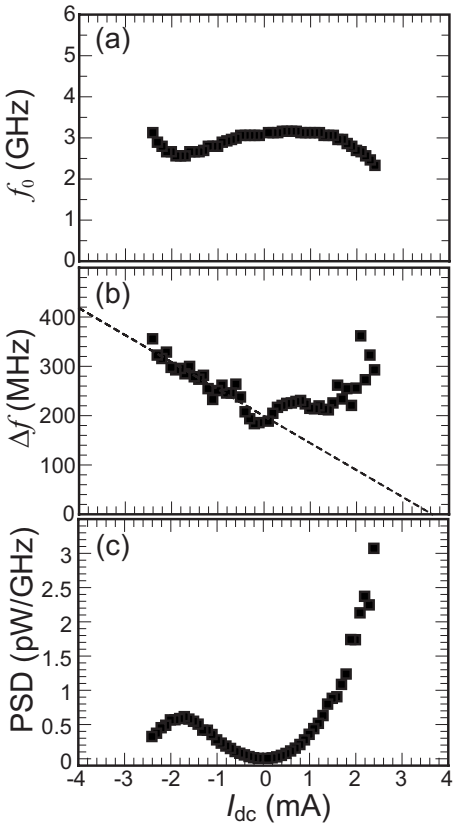

FIG. 5. Bias current (I_{dc}) dependence of (a) the peak frequency (f_0), (b) the linewidth (Δf), and (c) the PSD. The external magnetic field (H_{ext}) of 10 kOe was applied along the normal to the MTJ plane. The dashed line represents the result of a linear fit to the experimental data at $-2.4 \leqq I_{dc} \leqq 0.2$ mA.

crease in PSD with I_{dc} remains even at $I_{dc} > 1.7$ mA. This asymmetry of the I_{dc} versus PSD implies the contribution of the STT. Although the increment of PSD for the antidamping side is observed, the STT-induced rf oscillation is not achieved because the value of I_{dc} is lower than the estimated I_{c0}. In the measurement using other MTJs, the irreversible reduction in the device resistance was often observed around $I_{dc}=2.5$ mA (the bias voltage of ~750 mV), indicating the dielectric breakdown of the MgO barrier. $I_{dc} < 2.5$ mA is not sufficient to achieve STT-induced rf oscillation in this applied field direction. Consequently, in the present condition with the magnetic field applied strictly normal to the plane of the MTJ, a definite onset of the STT-induced rf oscillation is not observed.

IV. rf SPECTRA UNDER A MAGNETIC FIELD TILTED FROM THE NORMAL AXIS

As described in Sec. III, the application of a perpendicular magnetic field was effective in making the spectral shape a single peak structure although STT-induced rf oscillation was not achieved. This section shows the results when a magnetic field is slightly tilted from the normal axis of the plane of the MTJ. The tilt angle is a few degrees. Figure 6 shows a MR curve measured under a tilted magnetic field. While the

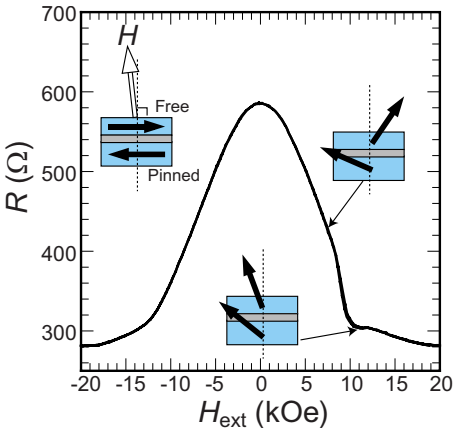

FIG. 6. (Color online) A MR curve measured under a perpendicular magnetic field which is slightly tilted from the normal to the plane of the MTJ. The tilt angle is a few degrees. The insets of the figure schematically illustrate the magnetic configurations before and after the in-plane magnetization switching. The black arrows denote the magnetizations of the free and the pinned layers.

shape of the MR curve in the negative field region is almost the same as that measured in the normal direction [Fig. 2(b)], an abrupt change in the resistance appears for $8 \leq H_{ext} \leq 10$ kOe. Considering the magnetization configuration (schematically shown in Fig. 6), the resistance change is attributable to the in-plane magnetization switching induced by the in-plane component of the tilted magnetic field.

Figure 7 displays RF spectra for (a) positive and (b) negative I_{dc}. H_{ext} was fixed at 11 kOe, which was the field after the in-plane magnetization switching. The positive bias current direction corresponds to the antidamping side whereas the negative one is the forced side. It is found that the peak intensities are clearly different between the positive and the negative bias current polarities. The peak intensity for the maximum positive bias current ($I_{dc}=2.3$ mA) is three orders of magnitude larger than that for the negative bias current ($I_{dc}=-2.3$ mA). In contrast to the variation in f_0 for the negative I_{dc}, which shows a gradual shift, f_0 for the positive

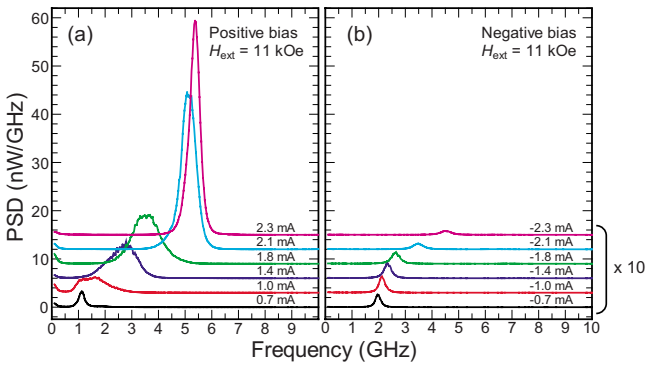

FIG. 7. (Color online) rf spectra measured at various bias currents (I_{dc}). The external magnetic field (H_{ext}) was set to 11 kOe. The magnetic field direction was tilted slightly from the normal to the plane of the MTJ. The current polarities are (a) positive and (b) negative. The spectra have been shifted vertically. The spectra for negative polarity have been magnified ten times for clarity.

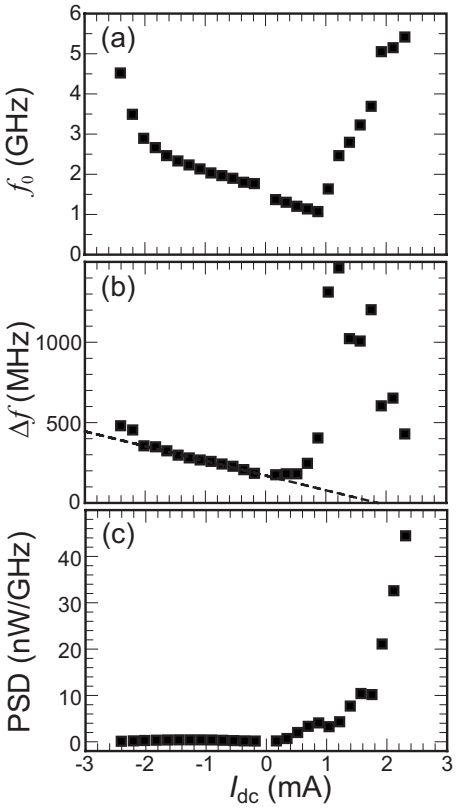

FIG. 8. Bias current (I_{dc}) dependence of (a) the peak frequency (f_0), (b) the linewidth (Δf), and (c) the PSD. The external magnetic field (H_{ext}) was set to 11 kOe. The magnetic field direction was tilted slightly from the normal to the plane of the MTJ. The dashed line represents the result of a linear fit to the experimental data at $-2.4 \leqq I_{dc} \leqq 0.2$ mA.

I_{dc} shows a discontinuous change together with peak broadening at $1.0 \lesssim I_{dc} \lesssim 1.8$ mA. Figure 8 summarizes (a) f_0, (b) Δf, and (c) PSD as a function of I_{dc}. f_0 varies linearly in the low I_{dc} region and shows a redshift (blueshift) on the antidamping (forced) side with I_{dc}. At high negative I_{dc}, a large blueshift occurs since STT on the forced side supports the intrinsic damping. On the other hand, f_0 for high positive I_{dc} also shows a remarkable blueshift with the discontinuous change in f_0 at $I_{dc}=1.0$ and 1.8 mA. At these values of I_{dc}, Δf also abruptly increases up to more than 1 GHz. Together with these abrupt changes in f_0 and Δf, PSD significantly increases. Using Eq. (3), I_{c0} is estimated to be ~ 1.8 mA by extrapolating the linear variation in Δf in the low I_{dc} region to zero [the dashed line in Fig. 8(b)]. This is almost the same as the value of I_{dc} at which PSD begins to increase drastically. Therefore, STT-induced rf oscillation is achieved at $I_{dc} > 1.8$ mA.

According to a theory of nonlinear auto-oscillators,[23] Δf above I_{c0} is given by,

$$\Delta f = \frac{I_{c0}\sigma}{2\pi}\frac{k_B T}{E_0}\left[1+\left(\frac{N}{\Gamma_{\text{eff}}}\right)^2\right], \tag{4}$$

where k_B is the Boltzmann constant, T is the absolute temperature, and E_0 is the average energy of the auto-oscillation. N is the nonlinear frequency shift which expresses the coupling between the oscillation frequency and the oscillation power. Γ_{eff} is the effective nonlinear damping. Equation (4) means that if the STT-induced rf oscillation exhibits a strong nonlinearity, Δf decreases in the nonlinear regime with increasing I_{dc} because of $N \neq 0$ and the increase in Γ_{eff} due to the effect of STT. At the boundary between the linear and nonlinear regimes, the theory also predicts line-shape distortion, which leads to the non-Lorentzian power spectrum near I_{c0}, and the spectral shape is recovered with increasing I_{dc}.[23] The experimentally observed drastic increase in Δf around I_{c0} and the following decrease in Δf are qualitatively similar to the tendency predicted by a theory for nonlinear auto-oscillators. However, the magnitude of the increase in Δf may be much larger than the theoretical prediction. Kim *et al.*[23] calculated Δf normalized by Δf at $I_{dc}=0$ (Δf_0) as a function of applied current and $\Delta f/\Delta f_0 \sim 0.5$ near I_{c0} was reported using typical parameters for the metallic multilayer. On the other hand, $\Delta f/\Delta f_0$ is obtained to be ~ 8.5 for the present results. It is unclear whether the theory of nonlinear auto-oscillators quantitatively explains the present results or not. Another mechanism might be required in order to explain the remarkable increase in Δf.

After the onset of STT-induced rf oscillation, f_0 shows a blueshift with the discontinuous change as I_{dc} increases. Since the magnetization direction of the free layer is almost out-of-plane due to the perpendicular magnetic field, the mode of the rf oscillation is considered to be an out-of-plane precession. The increase in the f_0 with I_{dc} is attributable to the change in the magnetization direction for the free layer due to the STT. The STT tilts the free layer magnetization away from the normal direction, which leads to the increase in the effective magnetic field. It is interesting that the rf oscillation is induced by applying the magnetic field at a tiny angle to the normal of the MTJ plane. One of the possible reasons is the difference in the relative angles between the two measurement conditions. Actually, the magnetization configuration for the tilted field condition is almost the parallel alignment whereas the relative angle for the normal direction case is 60° even at almost the same H_{ext}, leading to the different values of I_{c0}. The magnetic field angular dependence of the rf oscillation was also investigated using the point-contact devices[27,28] and it was reported that the lack of in-plane magnetic anisotropy led to the state of the complicated magnetization precession in the case of the perpendicular magnetic field. The in-plane component of magnetic field may be important to achieve the clear state of the STT-induced rf oscillation. This is another possible reason why the rf oscillation is not achieved at the magnetic field applied normal to the plane of the MTJ.

Figure 9 displays the rf spectra for $I_{dc}=1.8$, 1.9, and 2.3 mA in a logarithmic scale. The spectra for $I_{dc}=1.9$ mA shows another peak around 10 GHz, which is not observed for $I_{dc}=1.8$ mA. The peak frequency shifts with increasing I_{dc} to 2.3 mA and is twice as high as the frequency of the peak around 5 GHz. This means that the higher-frequency peaks correspond to the second harmonics of the peaks around 5 GHz. I_{dc} for the observation of the second-harmonic peak is in good agreement with I_{c0}. The maximum output power is calculated to be 26 nW at $I_{dc}=2.3$ mA tak-

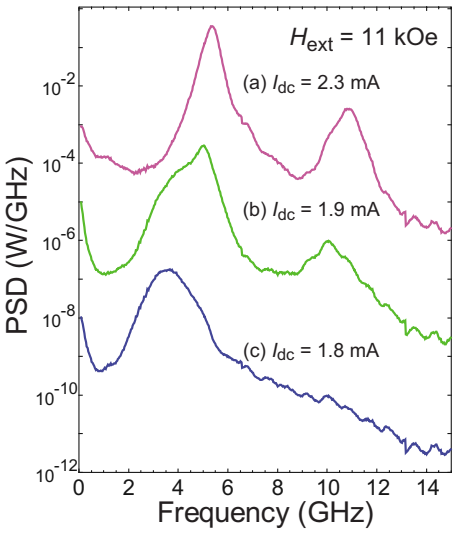

FIG. 9. (Color online) rf spectra plotted on a logarithmic scale. The bias current (I_{dc}) was set to (a) 2.3, (b) 1.9, and (c) 1.8 mA. The external magnetic field (H_{ext}) was fixed at 11 kOe. The magnetic field direction was tilted slightly from the normal to the plane of the MTJ. The spectra have been shifted vertically.

ing into account the rf output efficiency for the present device. A previous experiment for MgO-MTJs achieved a larger output power of 0.14 μW with applying the in-plane magnetic field.[13] The output power for the present study is reduced because both the free and pinned layer magnetizations are almost aligned in the perpendicular direction and the precession is an out-of-plane mode, which gives rise to a small resistance change. However, the present output power is still much larger than those reported for all-metallic multilayers.

Since the present measurement confirms the remarkable improvement in the spectral shape, the application of a perpendicular magnetic field is useful for the STT-induced rf oscillation of MTJs from the practical and fundamental points of view. In a previous paper using the in-plane magnetic field,[13] the precessional mode at the two ends of the long axis of the ellipsoidal pillar was observed in addition to the mode at the center of the pillar, leading to the multiple peaks in the rf spectra. On the other hand, the additional mode is suppressed owing to the perpendicular magnetic field, and single peak structures are obtained in the present study. The ratio of the power of the second harmonics to that of the fundamental peak (P^{2nd}/P^{Fund}) is $\sim$0.01 at I_{dc} =2.3 mA, which is much lower than other previous works using the in-plane magnetic field, e.g., $P^{2nd}/P^{Fund} \sim 13.5$ (Ref. 13). This low output power of the second harmonics indicates that the precessional angle is small even though the state of the rf oscillation is achieved. Although the application of the perpendicular magnetic field improves the spectral shape, Δf is still large. The minimum Δf is 170 MHz at I_{dc}=0.5 mA. After the onset of the rf oscillation, Δf is obtained to be 430 MHz at I_{dc}=2.3 mA, which is larger than those for metallic multilayers. The origin of the large Δf is an open question. Recently, the STT-induced rf oscillation was reported in the high-quality single-crystal Fe/MgO/Fe MTJs.[26] However, the minimum Δf was 200 MHz even for such single-crystal MTJs. On the other hand, the narrow Δf was reported in MTJs showing low junction resistance.[15] In order to understand the origin of the large Δf, further investigation is required.

V. CONCLUSION

We measured the rf spectra for CoFeB/MgO/CoFeB MTJs under a magnetic field applied perpendicular to the MTJ plane. Applying a perpendicular magnetic field was an effective way in making the shape of rf spectrum a single peak structure. This enabled us to precisely analyze the magnetic field and bias current dependences of the rf spectra. The rf spectra measured with the field applied strictly normal to the plane of MTJ were interpreted as behavior in the linear regime and STT-induced rf oscillation was not achieved in this magnetic field direction even when large bias currents were applied. On the other hand, a significant increase in PSD was observed with the magnetic field direction tilted slightly from the normal to the plane of MTJ. A remarkable broadening of Δf was also observed, which was qualitatively consistent with a theoretical prediction based on a model of nonlinear auto-oscillators. At I_{c0}=1.8 mA, PSD drastically increased and the second harmonics appeared, indicating the clear onset of STT-induced rf oscillation.

ACKNOWLEDGMENT

This work was partly supported by SCOPE program from MIC and grant-in-aid for scientific research from MEXT.

*go-sai@spin.mp.es.osaka-u.ac.jp

[1] J. C. Slonczewski, J. Magn. Magn. Mater. **159**, L1 (1996).
[2] L. Berger, Phys. Rev. B **54**, 9353 (1996).
[3] M. Tsoi, A. G. M. Jansen, J. Bass, W.-C. Chiang, M. Seck, V. Tsoi, and P. Wyder, Phys. Rev. Lett. **80**, 4281 (1998).
[4] S. I. Kiselev, J. C. Sankey, I. N. Krivorotov, N. C. Emley, R. J. Schoelkopf, R. A. Buhrman, and D. C. Ralph, Nature (London) **425**, 380 (2003).
[5] W. H. Rippard, M. R. Pufall, S. Kaka, S. E. Russek, and T. J. Silva, Phys. Rev. Lett. **92**, 027201 (2004).
[6] Q. Mistral, J. V. Kim, T. Devolder, P. Crozat, and C. Chappert, Appl. Phys. Lett. **88**, 192507 (2006).
[7] S. Kaka, W. H. Rippard, M. R. Pufall, S. E. Russek, T. J. Silva, and J. A. Katine, Nature (London) **437**, 389 (2005).
[8] F. B. Mancoff, N. D. Rizzo, B. N. Engel, and S. Tehrani, Nature (London) **437**, 393 (2005).
[9] S. I. Kiselev, J. C. Sankey, I. N. Krivorotov, N. C. Emley, M. Rinkoski, C. Perez, R. A. Buhrman, and D. C. Ralph, Phys. Rev. Lett. **93**, 036601 (2004).
[10] S. Yuasa, T. Nagahama, A. Fukushima, Y. Suzuki, and K. Ando,

Nature Mater. **3**, 868 (2004).
[11] S. S. P. Parkin, C. Kaiser, A. Panchula, P. M. Rice, B. Hughes, M. Samant, and S.-H. Yang, Nature Mater. **3**, 862 (2004).
[12] D. D. Djayaprawira, K. Tsunekawa, M. Nagai, H. Maehara, S. Yamagata, N. Watanabe, S. Yuasa, and K. Ando, Appl. Phys. Lett. **86**, 092502 (2005).
[13] A. M. Deac, A. Fukushima, H. Kubota, H. Maehara, Y. Suzuki, S. Yuasa, Y. Nagamine, K. Tsunekawa, D. D. Djayaprawira, and N. Watanabe, Nat. Phys. **4**, 803 (2008).
[14] A. V. Nazarov, K. Nikolaev, Z. Gao, H. Cho, and D. Song, J. Appl. Phys. **103**, 07A503 (2008).
[15] D. Houssameddine, S. H. Florez, J. A. Katine, J.-P. Michel, U. Ebels, D. Mauri, O. Ozatay, B. Delaet, B. Viala, L. Folks, B. D. Terris, and M.-C. Cyrille, Appl. Phys. Lett. **93**, 022505 (2008).
[16] K. Kudo, T. Nagasawa, R. Sato, and K. Mizushima, Appl. Phys. Lett. **95**, 022507 (2009).
[17] D. Houssameddine, U. Ebels, B. Dieny, K. Garello, J.-P. Michel, B. Delaet, B. Viala, M.-C. Cyrille, J. A. Katine, and D. Mauri, Phys. Rev. Lett. **102**, 257202 (2009).
[18] S. Cornelissen, L. Bianchini, G. Hrkac, M. Op de Beeck, L. Lagae, J. V. Kim, T. Devolder, P. Crozat, C. Chappert, and T. Schrefl, EPL **87**, 57001 (2009).
[19] K. Tsunekawa, D. D. Djayaprawira, M. Nagai, H. Maehara, S. Yamagata, N. Watanabe, S. Yuasa, Y. Suzuki, and K. Ando, Appl. Phys. Lett. **87**, 072503 (2005).
[20] C. Kittel, *Introduction to Solid State Physics*, 7th ed. (Wiley, New York, 1996).
[21] S. Yakata, H. Kubota, Y. Suzuki, K. Yakushiji, A. Fukushima, S. Yuasa, and K. Ando, J. Appl. Phys. **105**, 07D131 (2009).
[22] H. Kubota, A. Fukushima, Y. Ootani, S. Yuasa, K. Ando, H. Maehara, K. Tsunekawa, D. D. Djayaprawira, N. Watanabe, and Y. Suzuki, Appl. Phys. Lett. **89**, 032505 (2006).
[23] J. V. Kim, Q. Mistral, C. Chappert, V. S. Tiberkevich, and A. N. Slavin, Phys. Rev. Lett. **100**, 167201 (2008).
[24] A. N. Slavin and P. Kabos, IEEE Trans. Magn. **41**, 1264 (2005).
[25] S. Petit, C. Baraduc, C. Thirion, U. Ebels, Y. Liu, M. Li, P. Wang, and B. Dieny, Phys. Rev. Lett. **98**, 077203 (2007).
[26] R. Matsumoto, A. Fukushima, K. Yakushiji, S. Yakata, T. Nagahama, H. Kubota, T. Katayama, Y. Suzuki, K. Ando, S. Yuasa, B. Georges, V. Cros, J. Grollier, and A. Fert, Phys. Rev. B **80**, 174405 (2009).
[27] W. H. Rippard, M. R. Pufall, S. Kaka, T. J. Silva, and S. E. Russek, Phys. Rev. B **70**, 100406(R) (2004).
[28] W. H. Rippard, M. R. Pufall, and S. E. Russek, Phys. Rev. B **74**, 224409 (2006).